Khamdamov Giyos Makhmudovich
U.A. Arifov Institute of Ion-Plasma and Laser Technologies
2nd year PhD student
E-mail: khamdamovgiyos@mail.ru
Berdiyev Usmonjon Farmonovich
U.A. Arifov Institute of Ion-Plasma and Laser Technologies
Senior Researcher
E-mail: berdiyev@iplt.uz
Ashurov Rustam Khotamovich
U.A. Arifov Institute of Ion-Plasma and Laser Technologies
Senior Researcher
E-mail: r.ashurov@iplt.uz
Хамдамов Гиёс Махмудович
Институт ионно-плазменных и лазерных технологий им. У.А. Арифова
2-й курс докторант
E-mail: khamdamovgiyos@mail.ru
Бердиев Усмонжон Фармонович
Институт ионно-плазменных и лазерных технологий им. У.А. Арифова
Старший научный сотрудник
E-mail: berdiyev@iplt.uz
Ашуров Рустам Хотамович
Институт ионно-плазменных и лазерных технологий им. У.А. Арифова
Старший научный сотрудник
E-mail: r.ashurov@iplt.uz
Xamdamov G’iyos Maxmudovich
U.A. Arifov nomidagi ion-plazma va lazer texnologiyalari instituti
2-bosqich tayanch doktoranti
E-mail: khamdamovgiyos@mail.ru
Berdiyev Usmonjon Farmonovich
U.A. Arifov nomidagi ion-plazma va lazer texnologiyalari instituti

katta ilmiy hodim
E-mail: berdiyev@iplt.uz
Ashurov Rustam Xotamovich
U.A. Arifov nomidagi ion-plazma va lazer texnologiyalari instituti
katta ilmiy hodim
E-mail: r.ashurov@iplt.uz

# FABRICATION OF SILICON NANOPARTICLES BY PM400 MILLING AND THEIR SUITABILITY FOR LITHIUM-ION BATTERY ANODE.

**Abstract.** In this study, XRD and NanoSight analysis of silicon milled using a PM400 Ball Mill with 8 mm diameter balls in both aqueous and alcoholic media demonstrated an optimal particle size distribution and dispersion suitable for use as an anode material in lithium-ion batteries. The comparative study revealed that the milling efficiency depends on the type of solvent.

***Key words****: nanoparticle, silicon, mechanical grinding, anode material, XRD analysis, lithium-ion battery, solvent medium.*

# ИЗГОТОВЛЕНИЕ КРЕМНИЕВЫХ НАНОЧАСТИЦ МЕТОДОМ ИЗМЕЛЬЧЕНИЕМ PM400 И ИХ ПРИГОДНОСТЬ ДЛЯ ИСПОЛЬЗОВАНИЯ В КАЧЕСТВЕ АНОДОВ ЛИТИЙ-ИОННЫХ АККУМУЛЯТОРОВ.

**Аннотация.** В данном исследовании с помощью анализа рентгеновской дифракции (XRD) и системы NanoSight была исследована структура кремния, измельчённого в планетарной шаровой мельнице PM400 с использованием шаров диаметром 8 мм как в водной, так и в спиртовой среде. Результаты показали оптимальное распределение размеров частиц и степень дисперсии, подходящие для применения в качестве анодного материала в литий-ионных аккумуляторах. Сравнительный анализ выявил, что эффективность измельчения зависит от типа растворителя.

***Ключевые слова****: наночастицы, кремний, механическое измельчение, анодный материал, XRD-анализ, литий-ионный аккумулятор, среда растворителя.*

# PM400 TEGIRMONI YORDAMIDA KREMNIY NANOZARRALARINI OLISH VA ULARNING LITIY-ION BATAREYALAR ANOD MATERIALI SIFATIDA QO'LLASH.

**Annotatsiya.**Ushbu tadqiqotda 8 mm diametrli sharchalar yordamida PM400 Ball Mill (sharli tegirmon)da suvli va spirtli muhitda maydalangan kremniyning XRD va NanoSight tahlillari olib borildi. Natijalar shuni ko‘rsatdiki, bu usul orqali kremniy zarralari

litiy-ion batareyalarida anod materiali sifatida ishlatilishi uchun optimal zarracha o‘lchami taqsimoti va yaxshi dispersiyaga ega bo‘ladi. Solishtirma tahlil shuni ko‘rsatdiki, maydalash samaradorligi ishlatilgan erituvchi turiga bog‘liq.

***Kalit so‘zlar***: *nanozarrachalar, kremniy, mexanik maydalash, anod materiali, XRD tahlili, litiy-ion batareya, erituvchi muhit.*

## Introduction

Currently, there is a global energy crisis threat. As a result, the demand for renewable energy sources is sharply increasing. However, the main renewable energy sources are dependent on natural phenomena and do not have a continuous supply. This issue can only be resolved through the use of large-scale energy storage technologies [1]. There are many types of energy storage technologies available [2]. The main requirements for these energy storage batteries include the ability to store large amounts of energy, ecological safety, high discharge duration, and good adaptability. In the near future, among all existing energy storage technologies, vanadium redox flow batteries (VRFB) are considered promising due to their unique characteristics, such as independent power and energy storage capabilities, high charging capacity, and the ability of the electrolyte to support up to 20,000 cycles [3–5]. However, for high-energy-density portable storage systems, lithium-ion batteries (LiBs) remain the most viable solution. Among anode materials, silicon (Si) has attracted significant attention due to its extraordinarily high theoretical specific capacity of 3579 mAh $g^{-1}$, which is nearly ten times higher than that of conventional graphite anodes [6]. Despite this advantage, silicon’s large volume expansion (up to 280%) during lithiation causes mechanical stress, particle pulverisation, electrode delamination, and unstable solid electrolyte interphase (SEI) formation, all of which lead to rapid capacity fade [7].

To address these mechanical challenges, mechanical milling techniques, especially high-energy ball milling, have emerged as critical tools in the optimisation of silicon-based anodes. These methods aim to reduce silicon particle size, enhance homogeneity, and improve the structural integrity of the

electrode by creating better contact between active materials and conductive agents [8]. One common method is dry ball milling, where silicon powder is ground in the absence of a solvent. This approach is efficient for size reduction and helps induce nanostructuring. However, excessive dry milling can cause agglomeration, oxidation, and even amorphisation of silicon, which may negatively affect its performance [9].To overcome these limitations, wet milling techniques have been explored, where a solvent such as isopropanol or water is used as a dispersing medium during the milling process. Wet ball milling not only limits the temperature rise during grinding but also helps in forming more uniform dispersions and reducing oxidation. In particular, using aqueous media with appropriate surfactants or dispersants like Triton X-100 can stabilise particles and prevent re-agglomeration after milling [10].

Recent studies have shown that a two-step milling strategy is especially effective for composite silicon electrodes. In this optimised protocol, silicon and conductive carbon (e.g., Super C65) are first ball milled together in a dry or wet environment, while the polymer binder-such as poly(acrylic acid) (PAA)-is added afterward through magnetic stirring [11]. This separation of mechanical stress from the polymer prevents binder degradation, which often occurs when PAA is subjected to high-energy milling. For instance, high molecular weight PAA (450k and above) experiences significant chain scission during milling, resulting in weaker bonding to silicon and poorer electrochemical performance. By contrast, when the binder is added after milling, its molecular integrity is preserved, leading to improved electrode cohesion and longer cycle life [12]. Additionally, milling parameters such as time, frequency, and ball-to-powder ratio play a crucial role in the final electrode performance. Shorter milling times help reduce particle size without causing severe agglomeration, while extended milling may lead to increased defects and aggregation. Notably, the creation of nanoscale silicon domains through mechanical milling introduces grain boundaries that facilitate lithium diffusion, enhancing rate capability and capacity retention [9]. Laser diffraction and scanning electron microscopy

(SEM) analyses confirm that silicon particles after optimised ball milling exhibit a more controlled size distribution, improved contact with carbon networks, and a porous electrode architecture-favorable for electrolyte infiltration and SEI stabilisation. Electrodes produced using this strategy have demonstrated remarkable performance, retaining up to 84% of their initial capacity after 20 cycles, especially when using mid-range molecular weight PAA and optimised milling routines [11]. The present study aims to investigate the impact of different medium on the size of silicon.

The fabrication of silicon (Si) nanoparticles through mechanical milling has emerged as an effective strategy for developing high-performance anode materials for lithium-ion batteries (LIBs). While Si-based anodes offer significant advantages, such as a theoretical capacity of 4200 mAh/g—substantially higher than the 372 mAh/g of conventional graphite—they face critical challenges that hinder their practical application. These challenges include low electrical conductivity ($\sim 10^{-3}$ S $cm^{-1}$), slow lithium diffusion coefficients ($10^{-14}$–$10^{-13}$ $cm^2/s$), and substantial volume expansion ($\Delta V \sim 300\%$) during lithiation and delithiation, which can lead to rapid capacity fade and degradation of the anodes [1,2,3].

The solid-electrolyte interphase (SEI) layer, formed from the continuous reduction of the electrolyte on the anode surface, plays a crucial role in the performance of Si anodes. The SEI consists of both insoluble inorganic components, such as $Li_2CO_3$ and LiF, and partially soluble organic compounds. For optimal performance, the SEI must be mechanically stable, well-adhered to the anode, and able to accommodate volumetric changes during cycling. It should also be stable across the operating temperature range and potential window of the battery, while allowing lithium ions to pass through while blocking electron transfer [4,5].

To address the negative effects of uncontrolled SEI growth, strategies such as the use of electrolyte additives have been proposed [6,7]. Among various synthesis methods, planetary ball milling, particularly with PM400

mills, stands out as a cost-effective and scalable top-down approach for producing nanostructured Si powders with controlled sizes and morphologies. This method not only enhances cycling stability by reducing absolute volume changes but also shortens lithium-ion diffusion paths [8,9]. This study explores the optimization of milling parameters to produce Si nanoparticles.

## Experimental section

Raw metallurgical-grade silicon powder (≥98.6% purity, particle size <10 cm) was used as the starting material. Deionised water and ethanol (analytical grade) were utilised as the milling solvents. All materials were used as received without further purification.

Milling was conducted using a PM400 planetary ball mill (Retsch Gmbh, Germany) equipped with a 250 ml stainless steel milling jar and 8 mm diameter stainless steel balls. The silicon powder was subjected to wet ball milling under an ambient air atmosphere. Two different solvent systems were employed as a medium, deionised water and ethanol. For both solvent systems, the solid-to-liquid weight ratio was maintained at 1:5. Milling was performed at a rotational speed of 400 revolutions per minute (rpm) with a ball-to-powder weight ratio of 20:1. Each milling run was carried out for 12 hours.

After milling, the resulting slurries were poured into shallow trays and dried naturally at room temperature (~25°C) under air conditioning. No external heating or vacuum was applied during drying to minimise potential oxidation or structural changes. The dried powders were gently collected and stored in sealed containers for subsequent characterisation.

The crystal structure of the milled powders was characterised using X-ray diffraction (XRD) on a Bruker D8 Advance diffractometer with Cu Kα radiation ($\lambda$ = 0.154 nm). Data were collected over a $2\theta$ range of 10°–90° at a scanning rate of 0.02°/s. Crystallite sizes were estimated using the Scherrer equation based on the full width at half maximum (FWHM) of the primary diffraction peaks.

The particle size distribution of the milled powders was measured by nanoparticle tracking analysis (NTA) using a Malvern NanoSight NS300 instrument. Prior to analysis, powder samples were dispersed in the corresponding milling solvent and sonicated for 10 minutes to achieve uniform dispersion. Measurements were performed at room temperature.

## Results and discussion

Figure 1 displays the X-ray diffraction (XRD) pattern of the analysed sample, acquired using Cu-Kα radiation with a wavelength of 1.5406 Å. The diffraction peaks observed in the pattern correspond to the characteristic reflections of crystalline elemental silicon (Si), matched against the standard reference pattern (ICDD PDF No. 96-901-1999). The most intense peak appears at $2\theta \approx 28.45°$, which is attributed to the (111) crystallographic plane—a hallmark of the diamond cubic structure of silicon. Other observable peaks correspond to higher-index planes, indicating the presence of a well-ordered crystalline lattice.

The sharpness and symmetry of the peaks confirm the high crystallinity of the material, with no evidence of secondary phases or amorphous components. This confirms the successful synthesis or selection of phase-pure elemental silicon. The relative intensities and peak positions show excellent agreement with standard silicon diffraction data, reinforcing the material's structural fidelity and purity.

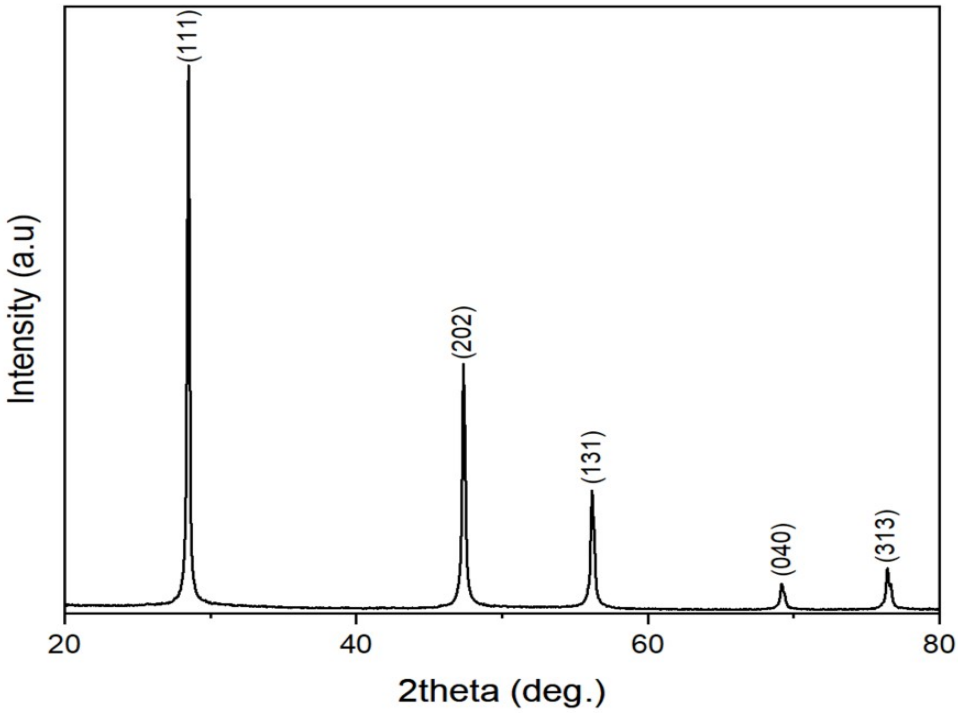


**Figure 1. X-ray Diffraction (XRD) Pattern of Elemental Silicon**.

Table 1 provides a detailed summary of the diffraction peaks identified in the XRD pattern shown in Figure 1. Each entry includes the 2θ position, calculated interplanar spacing (d-spacing), relative intensity, and the corresponding Miller indices (hkl) for the crystallographic planes. The dominant peak at 2θ = 28.45° with a d-spacing of 3.1355 Å corresponds to the (111) plane and is normalised to 100% relative intensity, serving as the primary orientation of the silicon lattice.

The table further lists additional peaks at 2θ values of 47.32°, 56.12°, 69.13°, 76.39°, and 88.02°, indexed to the (220), (311), (400), (331), and (422) planes, respectively. These planes are typical of elemental silicon and reflect the cubic crystal structure. The relative intensities of these reflections are categorised as moderate or low by the expected intensity distribution for silicon.

The tabulated data corroborate the results from the diffraction pattern, collectively verifying the identity, crystallinity, and purity of the sample as single-phase elemental silicon.

**Table 1.**

**Summary of XRD Peaks and Crystallographic Planes of Elemental Silicon (Si).NanoSight Analysis**

| No. | 2θ (°) | d-spacing (Å) | Relative Intensity | Miller Indices (hkl) |
|---|---|---|---|---|
| 1 | 28.45 | 3.1355 | 100% | (111) |
| 2 | 47.32 | 1.9207 | Moderate | (220) |
| 3 | 56.12 | 1.6375 | Moderate | (311) |
| 4 | 69.13 | 1.3577 | Low | (400) |
| 5 | 76.39 | 1.2459 | Low | (331) |
| 6 | 88.02 | 1.1086 | Low | (422) |

Figures 2a and 2b illustrate the nanoparticle tracking analysis (NTA) results for sample sets E6 and E7, respectively, with water serving as the dispersion medium for E6 and alcohol for E7. These plots provide detailed information on particle size distribution and concentration, where particle size (in nanometres) is shown on the x-axis, and concentration (in particles/mL) on the y-axis. Each coloured curve represents an independent measurement capture, demonstrating good reproducibility across replicates.

In Figure 2a**,** the NTA profile of sample set E6 (in water) reveals a dominant peak within the 100–200 nm range, with a maximum particle concentration of approximately $6.7 \times 10^6$ particles/mL. Secondary peaks appearing between 200–400 nm indicate a moderately polydisperse particle population. The inset provides a magnified view of the main peak, with the most abundant particle size measured at approximately 177 nm. The narrow confidence band in the inset highlights the consistency and reliability of the particle size distribution in water.

In contrast, Figure 2b shows the NTA results for sample set E7 dispersed in alcohol. This sample exhibits a shift toward smaller particle sizes, with the primary peak occurring between 80–140 nm and reaching a higher concentration of approximately $1.1 \times 10^7$ particles/mL, indicating a denser nanoparticle population than E6. A minor secondary peak is observed in the 200–300 nm range. The inset graph further emphasises the dominant particle size at

approximately 114 nm, with a narrow distribution range and minimal variance across captures.

Comparative analysis between the two samples suggests that the dispersion medium significantly influences nanoparticle size characteristics.

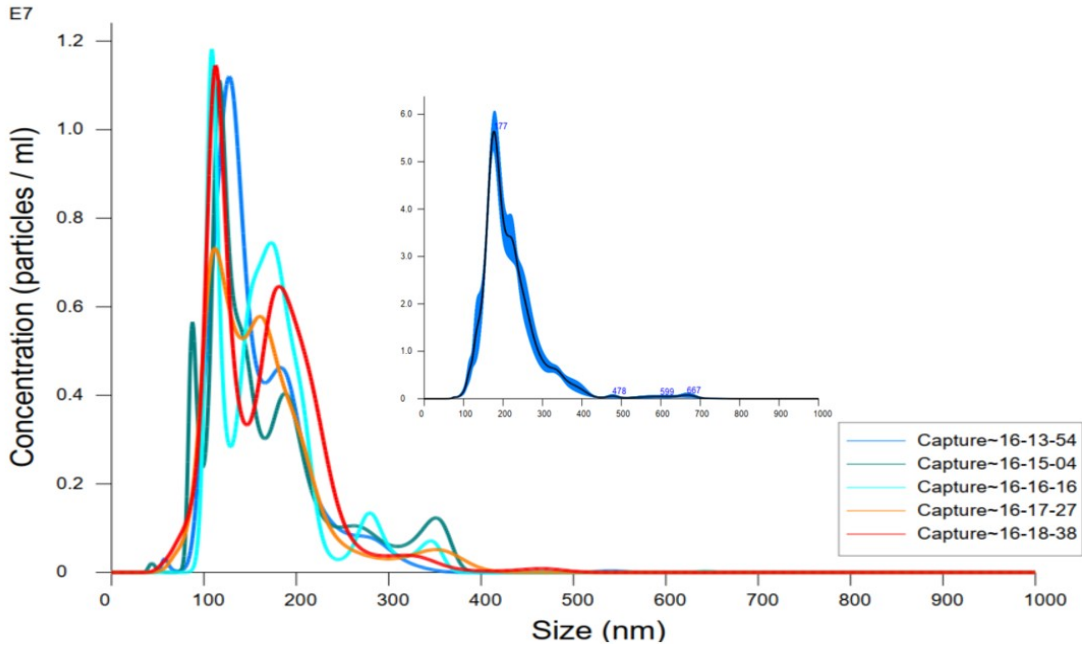


a

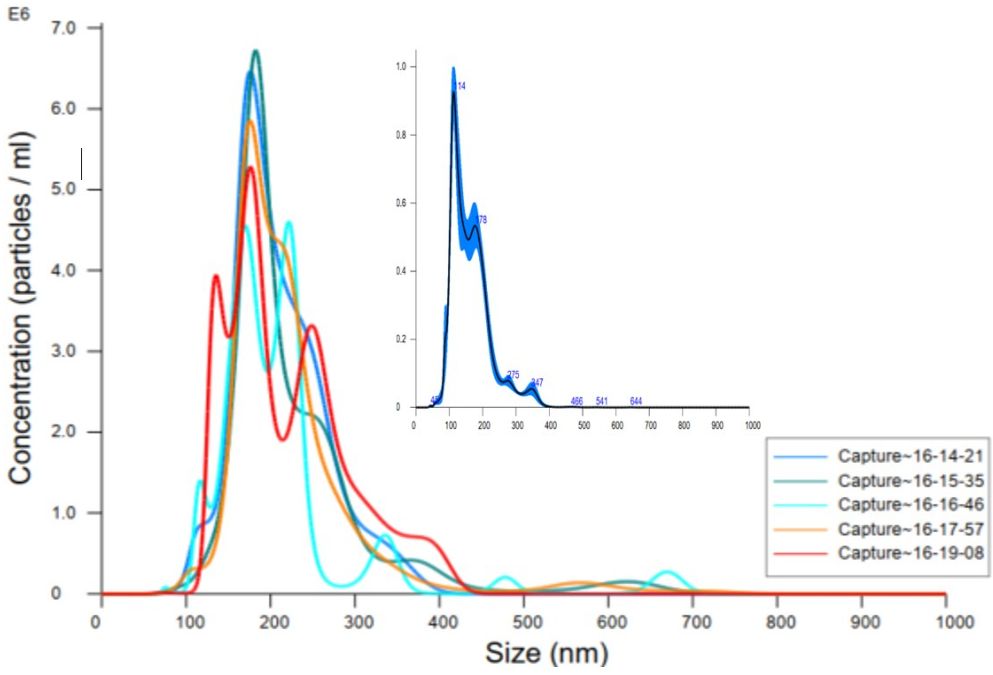


b

**Figure 2.** ***Nanoparticle Tracking Analysis (NTA) of Particle Size Distribution and Concentration in Sample Sets E6 (a, in water) and E7 (b, in alcohol).***

Specifically, alcohol as the medium in sample set E7 resulted in finer and more narrowly distributed particles compared to water in E6. This could be attributed to the lower surface tension and higher volatility of alcohol, which may promote better particle dispersion and reduce aggregation. These findings underscore the importance of solvent choice in nanoparticle preparation, particularly for applications in drug delivery, diagnostics, and nanomaterials where particle uniformity and size play a critical role in performance.

## Conclusion

This study explored the fabrication of silicon nanoparticles using a PM400 planetary ball mill with 8 mm diameter balls in both water and alcohol as milling media. The structural and size analyses, carried out through XRD and NanoSight (NTA), confirmed that the produced silicon powders possess the mostly crystalline purity and particle size distribution required for use as anode materials in lithium-ion batteries.

The results clearly show that several factors milling time, ball size, rotation speed, and especially the choice of solvent, play a major role in determining the final particle size and uniformity. Notably, milling in alcohol produced finer and more narrowly distributed silicon nanoparticles than milling in water. This suggests that the milling medium not only affects dispersion quality but also impacts the efficiency of the size reduction process itself.

By fine-tuning the milling parameters, we were able to produce silicon nanoparticles with characteristics that directly address some of the common challenges in lithium-ion battery anodes, such as large volume changes and slow lithium diffusion. The nanoscale size of the particles shortens lithium-ion pathways and helps accommodate structural expansion during cycling.

Overall, this work highlights that PM400 milling is not just a practical and scalable method**,** but also a versatile tool for tailoring silicon nanopowders to meet the growing demands of high-performance lithium-ion batteries.

## Literature

1. T. Chartrel, M. Ndour, V. Bonnet, S. Cavalaglio, L. Aymard, F. Dolhem, L. Monconduit and J. Bonnet, “Revisiting and improving preparation of silicon based electrode for lithium-ion batteries: Ball milling impact of poly(acrylic acid) polymer binder” Mater. Chem. Front. 3, 881-891 (2019), https://doi: 10.1039/c8qm00660a.
2. A. Guneren, A. Nada, A. Opalkova, K. Mosnackova, A. Kleinova, J. Mosnacek, and Z. Lences, “Novel alginate-based binders for silicon-graphite anodes in lithium-ion batteries: effect of binder chemistry on the electrochemical performance,” Journal of Applied Electrochemistry. 54, 1409-1423 (2024). https://doi.org/10.1007/s10800-023-02038-z.
3. A. Guneren, Z. Lences, “Statistical approach for the preparation of silicon-graphite anodes: The role of oxygen content and crystallite size on electrochemical performance,” Powder Technology. 443, 119982 (2024). https://doi.org/10.1016/j.powtec.2024.119982
4. H. Yang, S. Lin, A. Cheng, F. He, Z. Wang, Y. Wu, Y. Zhang, and X. Liu, “Recent Advances in Ball-Milling-Based Silicon Anodes for Lithium-Ion Batteries,” Energies. 16, 3099 (2023), https://doi.org/10.3390/en16073099.
5. Y. Zhen, A. Latief, and Y. Sheng, “Green Synthesis of Graphene Flake/Silicon Composite Anode for Lithium-Ion Batteries Using a Ball-Mill-Derived Mechanical Transfer Technique,” ACS Appl. Energy Mater. 7, 10574-10583 (2024), https://doi.org/10.1021/acsaem.4c02183
6. M. Cabello, E. Gucciardi, A. Herran, D. Carriazo, A. Villaverde and T. Rojo, “Towards a High-Power Si and graphite Anode for Lithium Ion Batteries through a Wet Ball Milling Process,” Molecules 25, 2494 (2020), https://doi:10.3390/molecules25112494.
7. S. Rousselot, M. Gauthier, D. Mazouzi, B. Lestriez, D. Guyomard, L. Roue, “Synthesis of boron-doped Si particles by ball milling and application in Li-ion batteries,” Journal of Power Sources 202, 262–268 (2012), https://doi:10.1016/j.jpowsour.2011.11.045.

8. J. Nzabahimana1, P. Chang, and X. Hu1, “Porous carbon-coated ball-milled silicon as high-performance anodes for lithium-ion batteries,” J Mater Sci 54, 4798–4810 (2019), https://doi.org/10.1007/s10853-018-3164-9
9. Ch. Shen, X. Fang, M. Ge, A. Zhang, Y. Liu, and Y. Ma, M. Mecklenburg, X. Nie, and Ch. Zhou, ACS Nano 12, 6280-6291 (2018), https://doi: 10.1021/acsnano.8b03312
10. W. Sun, R. Hu, M. Zhang, J. Liu, and M. Zhu, “Binding of carbon coated nano-silicon in graphene sheets by wet ball-milling and pyrolysis as high performance anodes for lithium-ion batteries,” Journal of Power Sources 318, 113-120 (2016), http://dx.doi.org/10.1016/j.jpowsour.2016.04.016
11. Y. Yang, X. Qu, L. Zhang, M. Gao, Y. Liu, and H. Pan, “Reaction_Ball-Milling-Driving Surface Coating Strategy to Suppress Pulverization of Microprticle Si Anodes,” ACS Appl. Mater. Interfaces 10, 20591-20598 (2018), https://doi: 10.1021/acsami.8b05609
12. Ch. Yim, F.Courtelb and Y.Lebdeh, “A high capacity silicon–graphite composite as anode for lithium-ion batteries using low content amorphous silicon and compatible binders,”. J. Mater. Chem. A 1, 8234–8243 (2013), https://doi: 10.1039/c3ta10883j